INTERNATIONAL ATOMIC ENERGY AGENCY
UNITED NATIONS EDUCATIONAL, SCIENTIFIC AND CULTURAL ORGANIZATION

INTERNATIONAL CENTRE FOR THEORETICAL PHYSICS
34100 TRIESTE (ITALY) - P.O.B. 586 - MIRAMARE - STRADA COSTIERA 11 - TELEPHONES: 224281/2/3/4/5/6
CABLE: CENTRATOM - TELEX 460392-I

SMR/98 - 48

AUTUMN COURSE ON GEOMAGNETISM, THE IONOSPHERE
AND MAGNETOSPHERE

(21 September - 12 November 1982)

TROPOSPHERIC RADIOPROPAGATION

S. RADICELLA

PRONARP
CAERCEM
Julian Alverez 1218
1414 Buenos Aires
Argentina

These are preliminary lecture notes, intended only for distribution to participants.
Missing or extra copies are available from Room 230.

3. TROPOSPHERIC RADIOPROPAGATION

3.1. Introduction

The propagation of the radio frequencies above 30 MHz and up to the optical band of the spectrum is strongly affected by the atmosphere. Several types of phenomena are observed due to its effects:

a) Refraction
b) Reflection from atmospheric layers
c) Scatter from irregularities of both neutral and ionized atmospheric gases
d) Duct propagation
e) Signal fading
f) Atmospheric water vapor and oxigen attenuation

The importance of each of these processes depends on the frequency range considered: b) and c) dominate in the 30-300 MHz band; a) and d) are important for the 300-3000 MHz portion of the spectrum; f) is the main attenuation mechanism of frequencies above 10 GHz; and e) is important all over the frequencies range.

This chapter will be mainly concerned with refraction and ductings effects in microwave propagation. Both are strongly controlled by variations of the meteorological parameters. The problem of heavy rain attenuation of microwaves will be also briefly considered.

It can be shown that, in a given point of the real atmosphere, the refractive index is function of the total pressure p, the absolute temperature T, and the partial pressure due to water vapor.

The values of n is of the order of 1.0003, and for practical reasons the "refractivity" N, given by:

$$N = (n - 1)\ 10^6, \qquad (1)$$

is introduced. Values of N are around 300.

The empirical relation of N adopted by the CCIR is:

$$N = 77.6 \times \frac{p(mb)}{T(°K)} + 3.73 \times 10^5 \frac{e(mb)}{T^2(°K)} \qquad (2)$$

In a real atmosphere the microwave ray does not follow a straight line, but travels along curved paths. For practical uses it is very important to introduce the concept of "effective earth radius" in order to restore rectilinear propagation over a terrain. The effective parameter is equal to K a_o , where K is the ratio of the effective radius to the actual radius. K is defined as a function of dN/dh:

$$K = \frac{1}{1 + a_o \frac{dN}{dh} 10^6} \qquad (3)$$

The "effective earth radius" is such that: a ray following a curved path over an earth of radius a_o is equivalent to a ray following a straight line over an earth of effective radius $a_{eff} = K\, a_o$ due to the height variation of the refractive index $\frac{dN}{dh}$.

From (3) the expression of dN/dh is:

$$\frac{dN}{dh} = \frac{77.6}{T}\frac{dp}{dh} - \frac{77.6p}{T^2}\frac{dT}{dh} - 7.5 \times 10^5 \frac{e}{T^3} + \frac{3.73}{T^2} \times 10^5 \frac{de}{dh} \qquad (4)$$

The first term at the right is always negative because p decreases with height. The following terms can be either positive or negative depending upon the meteorological conditions.

The refractivity N, in average, decreases with height with a value of 3.9 units per 100 m. This is the so called "standard value of refractivity gradient". When the gradient is greater than standard, the situation is named "superstandard refraction" and if dN/dh is smaller: "substandard refraction". The coefficient K of the effective earth radius, that is a function of dN/dh, has an average value of 1,33 for the standard refraction. Values of K above 1.47 correspond to superstandard refraction and values below 1.25 define the substandard condition.

An inversion of the refractivity gradient gives origin to the trapping or ducting of the radio wave. In such a case the microwave ray is guided in an atmospheric layer of specific meteorological conditions. Ducting occurs normally in the first 300 m above the ground and when its temperature is lower than the atmospheric temperature or when two adjacent air masses have different meteorological characteristics. This last situation is common in presence of cold or warm fronts irruptions. The more critical times of the day are sunrise and sunset hours when elevated duct due to heating from below and near ground ducts due to cooling from below, are common.

For comparison reasons refractivity N measured at ground level is normally reduced to its sea level value N_0 considering an average exponential atmosphere. The CCIR gives world maps of this value in his Report 563-1. The same document also displais maps of ΔN, that is a measure of the refractivity gradient, equal to $Ng-N_{1km}$, where N_{1km} is the value at an height of 1 km or at the isobar of 850 mb for a standard atmosphere. It must be noticed that ΔN is not reduced to sea level height.

When microwaves above around 10 GHz are used in telecommunications the accurence of rain is a common source of irregular attenuation. Water vapor along the path and liquid water like fog or low clouds are also sources of signal strenght variations. Rain effects are analyzed using the so called "rain rate" and "surface point rain rate" obtained from statistics of meteorological data, because there is no theorethical basis for the calculation of rainfall. The rain rate is measured as the water fallen in mm of rain per unit of time. For radio propagation purposes the desired rain rate is the almost instantaneous one but, in reality, only very few places in the world do make such type of measurements. Available data are the long duration rain accumulation hourly, daily or annual, and the data on rain rate averaged over time intervals of about 5 minutes, for a much more limited number of locations. The rain rate distribution is usually aproximated by either of two empirical laws according to the intensity of the rainfall. For light and moderate rain the log normal distribution, Battesti (1979a), has been used while for heavy rain the gamma law is usually applied (Morita and Higuti, 1976, Boithias, 1980).

Recently a new method was described for estimating the rainfall distribution (Morita 1980). The data were divided into two portions (for light and heavy rains) and each of them was approximated by log-normal distributions with different adjusting parameters. Also, for Canadian data (Segal, 1980) a power law was used to fit them.

Unfortunately nature is not so mathemathicaly inclined, therefore Hirsch and Romanelli (1982) proposed an empirical rain rate distribution in order to describe more realistically rainfall data.

This distribution (the polylog normal distribution) is given by:

$$P(R) = \frac{1}{2} \exp\left(-\left(\sum_{n=0} a_n (\log R_T')^n\right)^2 /2\right) \; d(\log R_T') \qquad (5)$$

where R_T stands for rainfall rate in a given time interval T and the a_n are obtained by the least square methods. When only the first two coefficients are used the log-normal distribution is obtained. Fig. 3.0 shows rainfall distributions data for Buenos Aires, Iguazú and Río de Janeiro (Romanelli and Hirsch, 1982; private communication. Pontes and Assis 1981). Also shown is a typical gamma distribution. Because the ordenate is the inverse of the normal distribution a log-normal one would be represented by a straight line. Otherwise a polynomial in log R can be used to approximate data using the equation given above.

Pontes and Assis (1981) have noted that rainfall data for Río de Janeiro (Tropical maritime, wet-and-dry climate) display a large year-to-year variation. For example: at 10^{-3} of the time this variation is ± 50 mm/h. Romanelli and Hirsch (1982) using data from Iguazú and Buenos Aires (Sub-tropical-humid climate) show that the year-to-year variation also for 10^{-3} of the time is ± 12 mm/h and only ± 6 mm/h, respectively. These results indicates a strong climatic control of the rain rate variability.

To estimate attenuation along the path for a radio link it is necessary to know the specific rain rate at each point, that is related to the instantaneous rain rate through the raindrop sizes distribution. It must be taken into account that most of the meteorological data are point data and that the pointfield is not adecuate for radiopropagation purposes. Some kind of prediction of attenuation can be made in a regional scale as it has been shown by Crane (1980). Fig. 3.1 show the world map of rain rate climate regions given by him. To each zone correspondes a type of rain rate distribution that can be expressed as rain rate R in mm/h as a function of percent of year the rain rate is exceeded. Fig. 3.2 displays the model distribution for the different climatic regions found in South America. It is easily seen that the continent has a large variety of rain rate distribution. The same figure shows the actual 5 min interval rain rate distribution for Iguazú and Buenos Aires (Romanelli and Hirsch, 1982).

The signal attenuation in dB as a function of rain rate and distance is given by (Crane, 1980):

$$A\ (Re_p,\ D) = aR_p^b\ \left(\frac{e^{ubD} - 1}{ub}\right) \qquad (6)$$

Where Rp is the surface-point rain rate in mm/h, D the path distance and x, p and u are empirical constants. The specific attenuation in dB/km is related to the point rain rate by

$$A = aR_p^b \qquad (7)$$

The parameters a and b have been calculated by Olsen et al. (1978) for differents temperatures and drop size distribution.

The most widely used drop size distribution are(Olsen et al, 1978):

a) Laws-Parsons:
Which has been found to be a reasonable choice for mean drop size spectrum in continental temperature rainfall. This distribution is itself divided into two ranges. Low: for averages rain rates of 50 mm/h and High: for rain rates exceeding this value.

b) Marshall-Palmer:
It has been found to be most applicable to widespread rain in continental temperature climates, although it has a tendency to overestimate the number of small drops.

c) Thunderstorm (distribution of Joss et. al)

d) "Drizzle" distribution of Joss et al.

3.2. Tropospheric propagation in South America:

In this chapter values of refractivity for different locations in South America, using results from Panaccio et al (1970) and Pontes and Assis (1981), are discussed. The analysis can be considered representative for several of the climatic regions of the continent (Table 3.1.).

Fig. 3.3. show refractivity reduced at sea level, No, as a function of latitudes between 55° and 20°S, for February and August, 12.00 LT and 00.00 LT (data from Panaccio et al, 1970). Fig. 3.4. displays the same parameter for latitudes between 0° and 25°S for 12.00 UT (data from Pontes and Assis (1981)).

The observed variations are in good agreement with the world maps of No given in CCIR Report 563-1. The latitudinal behaviour observed in Brasil and Argentina are consistent in showing the importance of the climatic conditions on the values of No.

The equatorial climate site of Belem displays large values of refractivity without much seasonal changes in accordance with the high values of temperature and humidity throughout the year. The tropical and subtropical sites of Campo Grande, Rio de Janeiro, Curitiba, Salta, Resistencia, Córdoba and Ezeiza, show large values of No and important seasonal changes, both decreasing with latitude, following the temperature and water content excursions typical of those climatic areas. The southern sites of Comandante Espora and Comodoro Rivadavia display low values of refractivity in good agreement with the decreasing temperature with latitude and the semiarid condition of that region. Ushuaia shows a small increase of No in accordance with the rainy climate of the area.

Fig. 3.5. displays the variation of N in the first 1 km above the surface N, using data from Panaccio et al. (1970). Its seasonal and latitudinal variations are roughly similar to those of No in accordance with the meteorological conditions. The relatively low values obtained at Salta (1226 m above sea level) and at Córdoba (476 m) are related to the fact that N is computed from N measured at the ground surface without reducing it to sea level like is done for No.

Fig. 3.6. gives the more probable values of the effective earth radius coefficient K at noon as a function of latitude (from Panaccio et al.,1970). The low values for Salta and Córdoba are again related to their altitude above sea level. The general tendency to decrease with increasing latitude is in agreement with the values of N shown in fig. 3.5. taking into account that K is a function of dN/dh.

Finally, fig. 3.7. shows the dominant refraction condition in percentage of time. At low latitudes, in subtropical and temperate areas, the refraction is most of the time superstandard and standard and in areas with lower temperature and water vapor content the dominant refraction is standard and substandard.

Table 3.2., taken from Pontes and Assis (1981), gives percentage of time of occurence of ducts for the Brasilian sites, including the island of Trinidade, in the Atlantic Ocean. It can be seen that the coastal or oceanic equatorial and tropical sites of Belem, Rio de Janeiro and Trinidades displays ducts occurence during all the year. The remaining inland sites are almost free of ducting conditions.

The Grupo de Radiopropagación of the Universidad Nacional de La Plata, integrated in the National Programme of Radiopropagation of Argentina, has developed, following a request from the Secretary of Communications, a set of computer programs in BASIC lenguage to calculate field strenght attenuation, minimun effective height of antenna and reflection coefficient, for different kinds of surface and paths over a flat earth. The equivalent programs for spheric earth are being tested.

Calculation and measurements have been made of specific rainfall attenuation of microwaves by Pontes and Assis (1981) for Rio de Janeiro and calculations were performed by Romanelli and Hirsch (1982) for Iguazú and Buenos Aires. Fig. 3.8. show specific attenuation values for 10 GHz computed using actual rainfall distributions. For Rio de Janeiro a and b coefficients are those obtained from Laws-Parsons (high) distributions, and for Iguazú and Buenos Aires the Laws-Parsons (low) distribution was used.

3.3 Figure Captions

Fig. 3.0. Cumulative rainfall distribution (log R) for Buenos Aires, Iguazú and Río de Janeiro in percentage of time exceeded by the ordinate/ inverse of the tail of the normal distribution Q (see text).

Fig. 3.1. World map of rain rate climate regions, from Crane (1980).

Fig. 3.2. Rain rate model distribution for the different climatic regions found in South America from Crane (1980). Actual rain rate distribution for Iguazú and Buenos Aires are also shown.

Fig. 3.3. Refractivity, reduced at sea level, Ro, as a function of latitude in Argentina, for February and August and 12.00 LT and 00.00 LT.

Fig. 3.4. Refractivity reduced at sea level, Ro, as a function of latitude in Brasil, for February and August at 12.00 UT.

Fig. 3.5. Variation of refractivity in 1 km, ΔN, as a function of latitude in Argentina, for February and August and 12.00 LT and 00.00 LT.

Fig. 3.6. More probable value of the effective earth radius coefficient K at noon as a function of latitude in Argentina.

Fig. 3.7. Dominant refraction condition in percentage of time as a function of latitude in Argentina.

Fig. 3.8. Specific rain attenuation values in percentage of time exceeded by the abcissa for Río de Janeiro, Iguazú and Buenos Aires (f = 10 GHz, Rain temperature 20°C) (see text).

3.4. References

BATTESTI, J. (1979a) "Effet des hydrométéores sur la propagation des ondes aux frequences superieures a 10 GHz"; CNET, Note Technique NT/TCR/APG/63.

BOITHIAS, L. (1980) "Au sujet de la Loi de distribution statistiques des intensites de pluie"; Ann. Telecommunic. 35, 365.

CRANE, R.K. (1980) "Prediction of attenuation by rain", IEEE Transactions on Communications, COM-28, 1717.

HIRSCH, F. and ROMANELLI, L. (1982) "Generalización de una ley empírica aplicable a problemas geofísicos", presented at the XII Scientific Meeting of the Asociación Argentina de Geofísicos y Geodestas.

MORITA, K. (1980) "A new method for estimating rain attenuation distribution"; Rev. of Elect. Communic., 28, 472.

OLSEN. R.L.; ROGERS, D.V. and HODGE, D.B. (1978) "The a R^b relation in the calculation of rain attenuation", IEEE Transactions on Ant. and Prop. , AP-26, 318.

PANACCIO, L.A.; LABORERO, R.L.; RIZZO, F.P. and VINACUR, F.S. (1970) "Estudio del índice de refracción en la República Argentina" ; ENTEL-Argentina, Buenos Aires.

PONTES, M.S. and ASSIS, M.S. (1981) "Propagation conditions in South and Central América", presented to the preparatory Seminar for 1983 RARC.

ROMANELLI, L. and HIRSCH, F. (1982) "Distribución de lluvias en Buenos Aires e Iguazú", to be published.

SEGAL, B. (1980) "An analytical examination of mathematical models for the rainfall rate distribution function"; Ann.Telecomm. 35, 434.

TABLE 3.1.

UPPER AIR PARAMETERS

METEOROLOGICAL STATION	GEOG. LAT (°S)	GEOG. LONG (°W)
BELEM (BRAZIL)	1.46	48.48
CAMPO GRANDE (BRAZIL)	20.46	54.67
SALTA (ARGENTINA)	21.85	65.48
RIO DE JANEIRO (BRAZIL)	22.90	43.17
CURITIBA (BRAZIL)	25.52	49.17
RESISTENCIA (ARGENTINA)	27.47	58.98
CORDOBA (ARGENTINA)	31.32	64.22
EZEIZA (ARGENTINA)	34.83	58.53
SANTA ROSA (ARGENTINA)	36.58	64.27
COMANDANTE ESPORA (ARGENTINA)	38.73	62.17
COMODORO RIVADAVIA (ARGENTINA)	45.78	67.50
USHUAIA (ARGENTINA)	54.80	68.32

TABLE 3.2

OCCURRENCE OF DUCTS

Meteorological station	Percentage of time												
	Jan	Feb	Mar	Apr	May	Jun	Jul	Aug	Sep	Oct	Nov	Dec	Annual mean
Belém	13.0	14.0	21.0	12.8	11.1	11.9	16.1	9.2	24.0	22.2	30.3	250	16.3
Rio de Janeiro	15.4	16.0	19.2	19.7	8.5	7.3	12.3	11.7	10.3	16.1	14.9	14.8	14.1
Campo Grande	-	-	-	-	-	-	-	-	-	-	-	-	-
Curitiba	2.1	-	4.6	-	-	-	-	-	-	-	2.7	1.2	1.2
Trindade Island	52.5	46.5	56.0	38.0	36.0	12.5	9.0	11.5	13.5	20.0	No data	No data	-

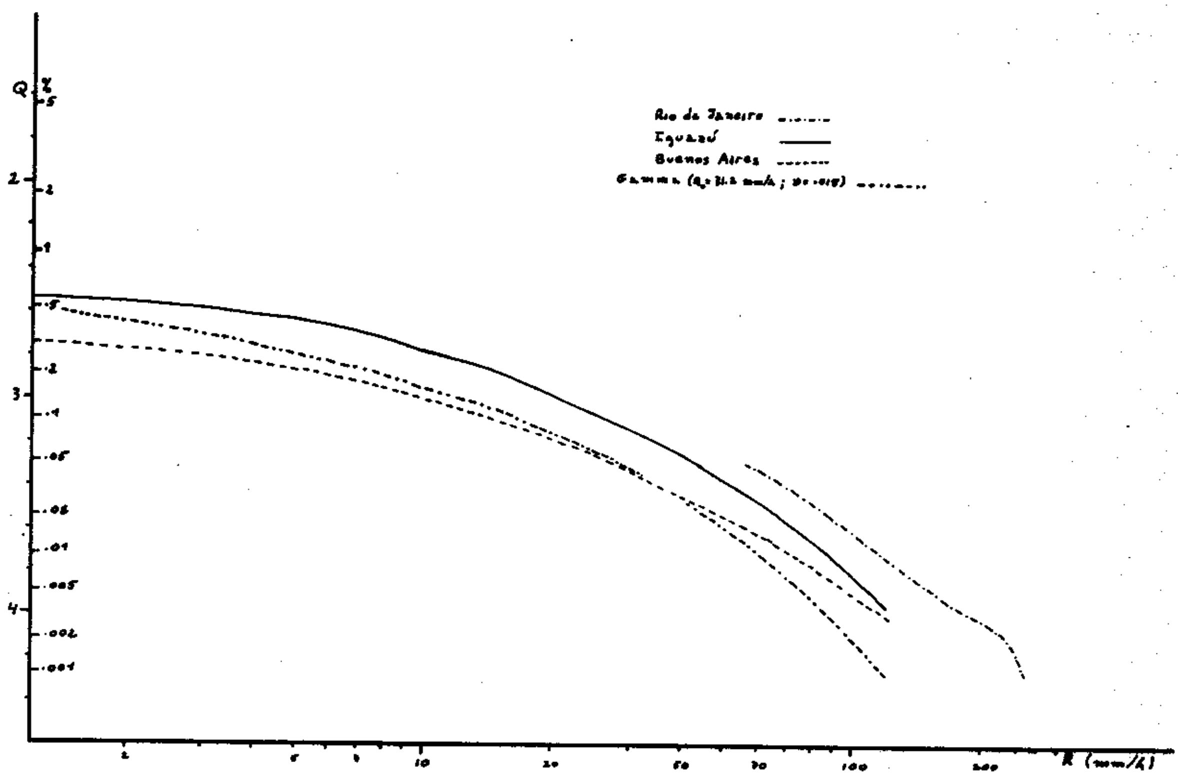

Fig. 3.0

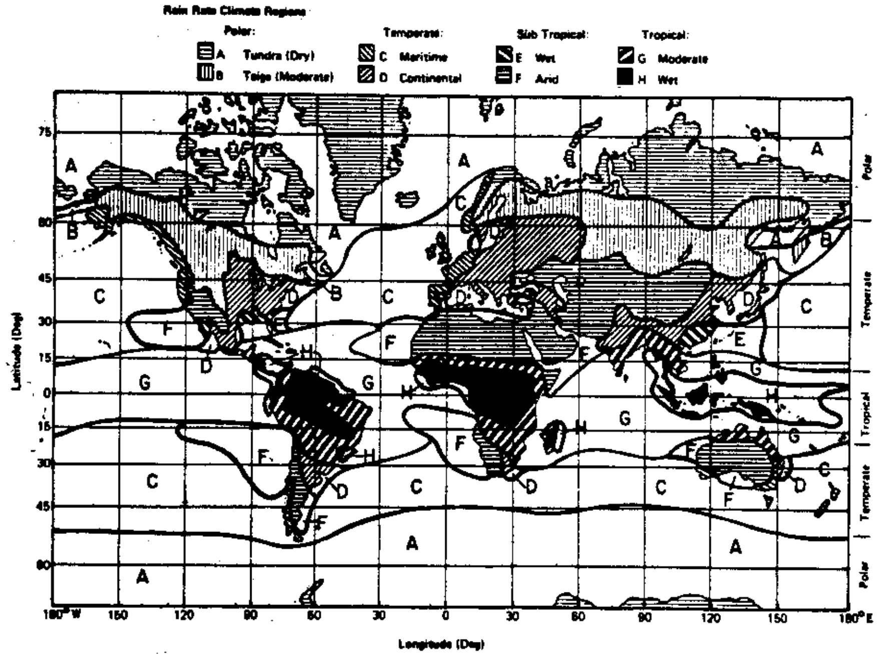

Rain Rate Climate Regions
Polar:
A Tundra (Dry)
B Taiga (Moderate)
Temperate:
C Maritime
D Continental
Sub Tropical:
E Wet
F Arid
Tropical:
G Moderate
H Wet
Latitude (Deg)
Longitude (Deg)
Polar
Temperate
Tropical

Fig. 3.1

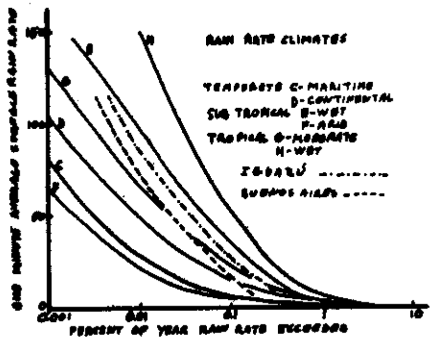

RAIN RATE CLIMATES
TEMPERATE C-MARITIME
D-CONTINENTAL
SUB TROPICAL E-WET
F-ARID
TROPICAL G-MODERATE
H-WET
PERCENT OF YEAR RAIN RATE EXCEEDED

Fig. 3.2

COINDICE DE REFRACCION No EN FUNCION
DE LA LATITUD
(REPUBLICA ARGENTINA)

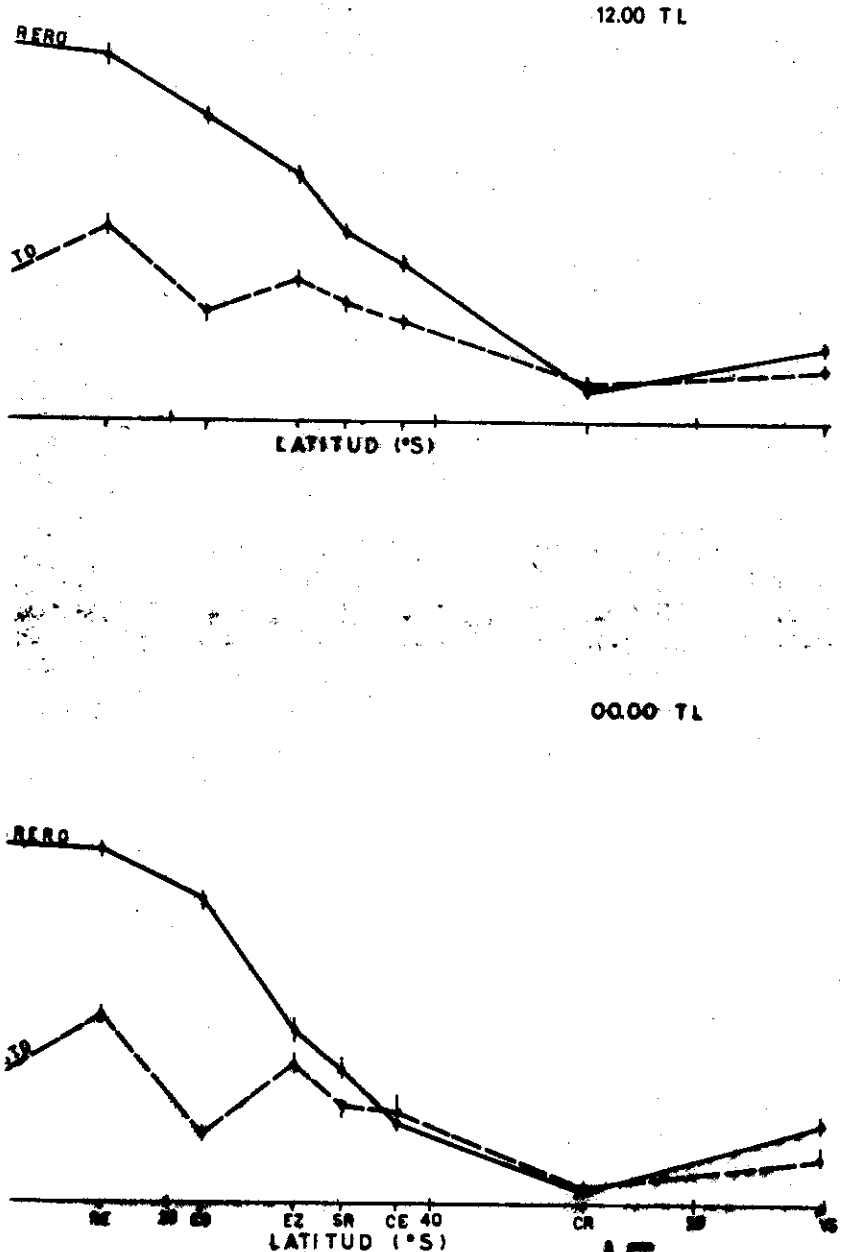

Fig.3.3

COINDICE DE REFRACCION No EN
FUNCION DE LA LATITUD
(BRASIL)

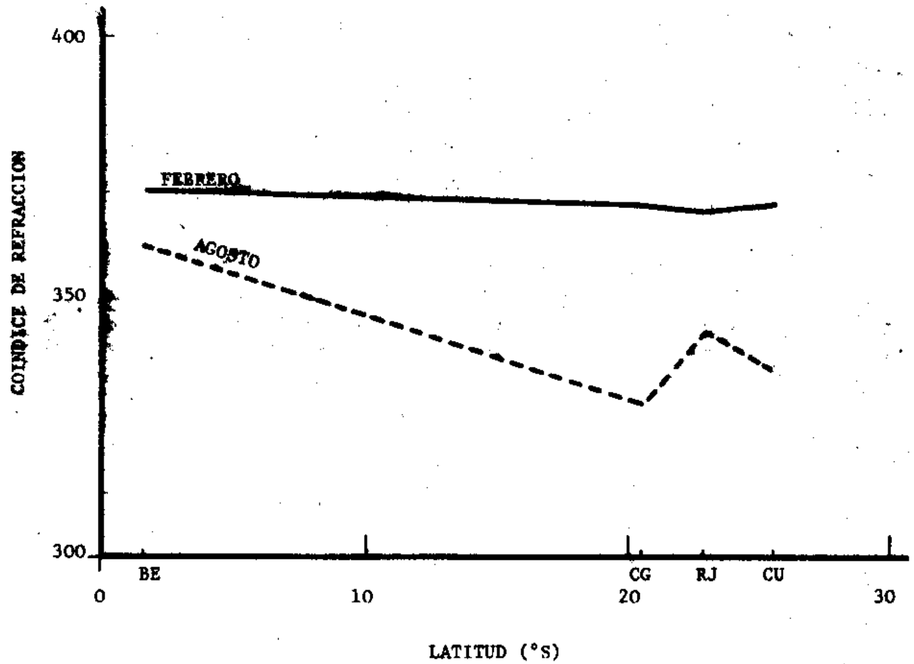

Fig. 3.4

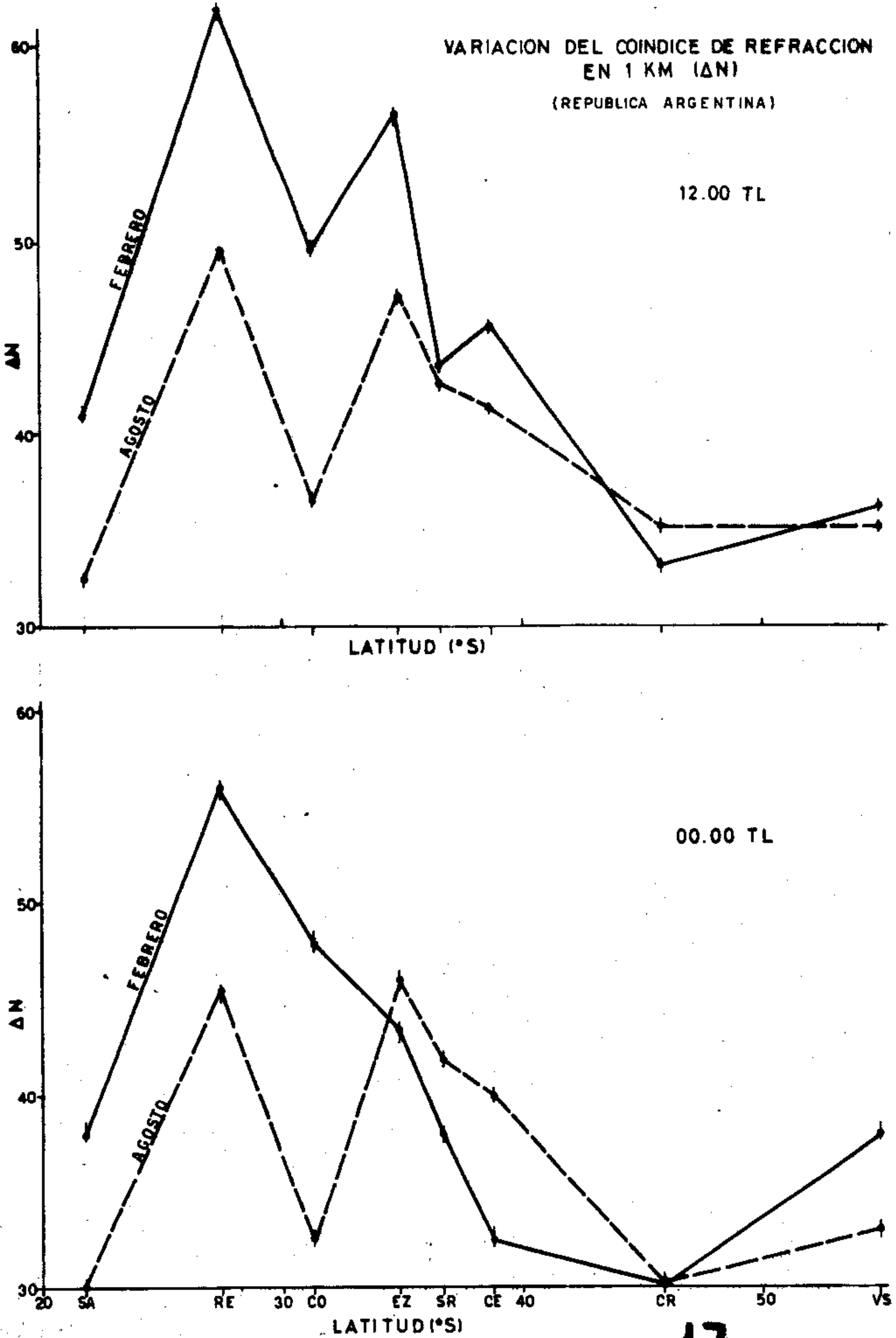
VARIACION DEL COINDICE DE REFRACCION
EN 1 KM (ΔN)
(REPUBLICA ARGENTINA)
12.00 TL
FEBRERO
AGOSTO
ΔN
60
50
40
30
LATITUD (°S)
00.00 TL
FEBRERO
AGOSTO
ΔN
60
50
40
30
20
SA
RE
30
CO
EZ
SR
CE
40
CR
50
VS
LATITUD (°S)

Fig. 3.5

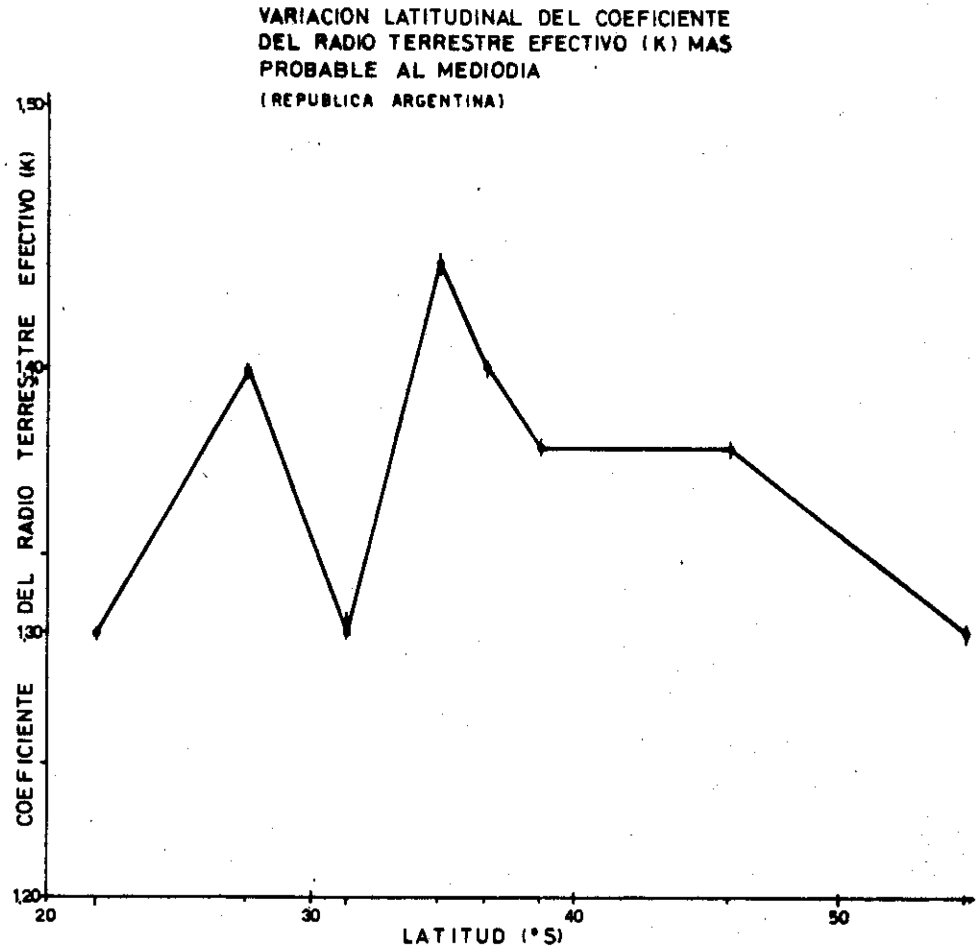
VARIACION LATITUDINAL DEL COEFICIENTE
DEL RADIO TERRESTRE EFECTIVO (K) MAS
PROBABLE AL MEDIODIA
(REPUBLICA ARGENTINA)
COEFICIENTE DEL RADIO TERRESTRE EFECTIVO (K)
1,50
1,40
1,30
1,20
20
30
40
50
LATITUD (°S)

Fig. 3.6

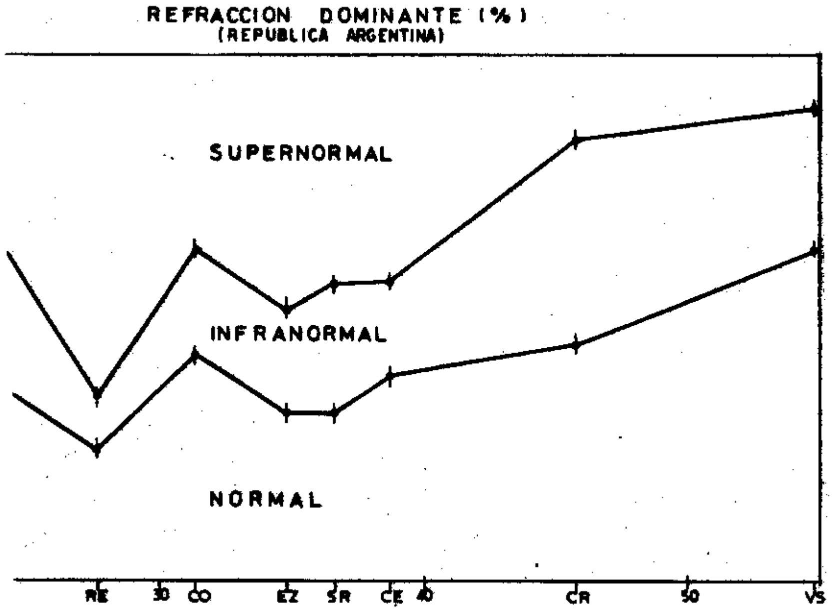

Fig. 3.7

19

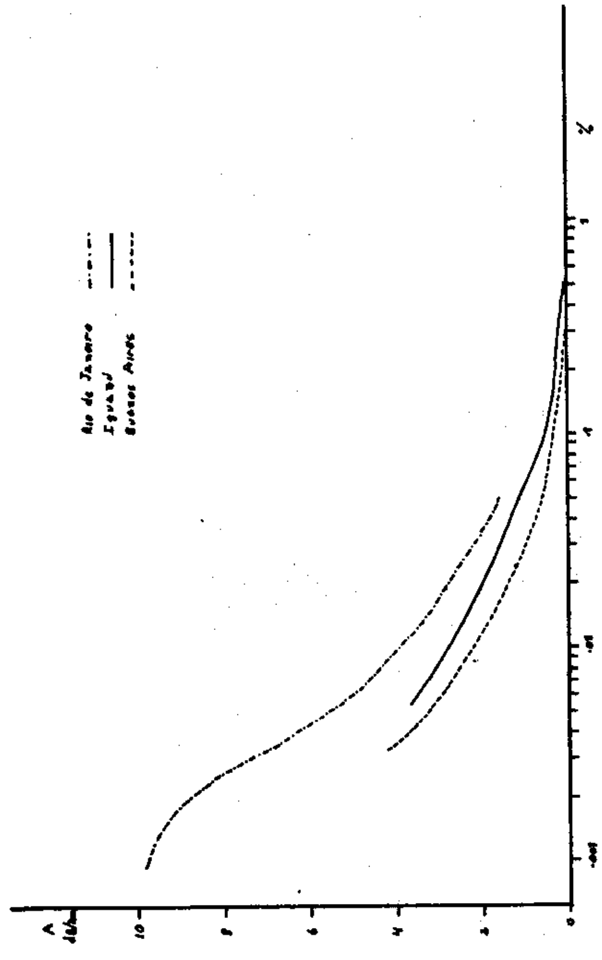

Fig. 3.8

20